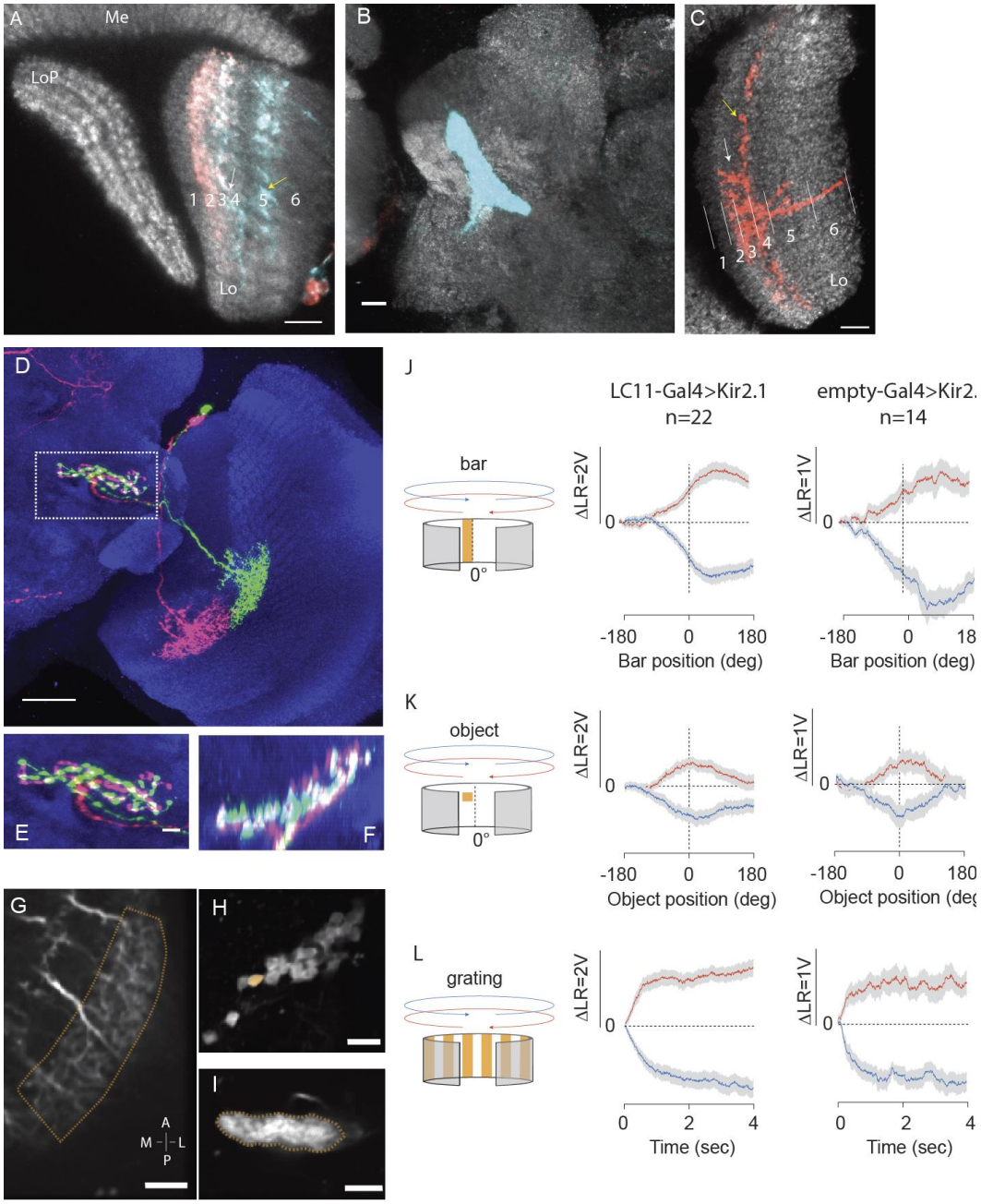

Figure S1 related to Figure 1: A-C) Pre and post synaptic organization of LC11 in the Lobula. A) R22H02-Gal4 shows pre-synaptic labeling in the lobula. Dorsal view of R22H02-Gal4 driving the expression of dendritic marker UAS-DenMark (red) and pre-synaptic marker UAS-Syt-EGFP (cyan) in lobula (gray). Yellow arrowhead indicates the layer (5) only innervated by LC11 and white arrowhead indicates the layers innervated by both LC11 and Loi. Both layers show pre-synaptic labeling (cyan). B) Dorsal view of VLPR and LC11 glomerulus labeled with pre (cyan) and post (red) synaptic markers. C) R22H02-Gal4 labels LC11 and Lobula intrinsic neurons (Loi). Stochastic labeling R22H02-Gal4 driver revealed two cell types in lobula. LC11 (red, white arrowhead) innervates layers 2,3,4, and 5 (neuropile in gray), whereas Lois (red, yellow arrowhead) innervates the border of 3rd and 4th strata in lobula (compare with Figure 1C). All scale bars are 10 um and layer identification is based on [S7]. D-F) Multicolor stochastic labeling of LC11. D) Anterior view of two LC11s tagged with HA (green) and FLAG (red). Dashed

rectangle indicates the glomerulus. Scale bar is 25 um E) Anterior view of LC11 glomerulus modified from D. F) Dorsal view of two LC11s innervating VLPR. Image is modified from D. Scale bar is 10 um in F and E. G-I) Representative images of 2 photon calcium imaging experiments illustrating extracted region of interests (ROIs) from different cellular compartments. G) Example dendritic ROI is shown. Orange dashed border represents the included pixels for analysis. H) Example cell body ROI is shown. Orange region represents a single cell body and extracted pixels for analysis. I) Example glomerular ROI is shown. Orange dashed line represent included pixels for analysis. Anatomical reference is provided with following letters: A: Anterior, P: Posterior, M: Medial and L: Lateral. Scale bars are 10 um. J-L) Effects of blocking LC11 on steering responses to bar, object, and full-field gratings. Mean response traces are color coded for stimulus direction and shaded region indicates ± S.E.M.

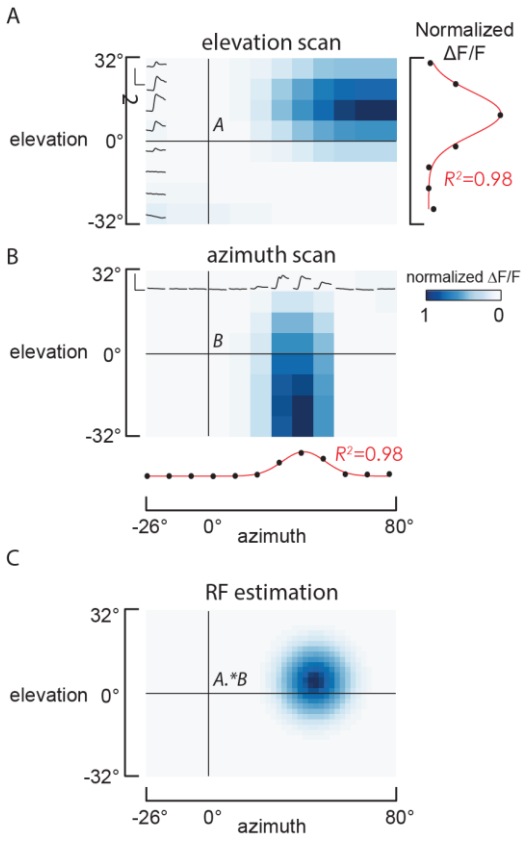

Figure S2 related to Figure 2: Receptive field reconstruction. A and B) Responses of a single LC11 to an 8.8° square object swept at 8 different trajectories (right side of the heatmap) on both axis. Data then downsampled and a matrix for each axis was generated and represented as a heatmap. The two matrices were multiplied and a Gaussian curve was fit (red) to both axes in the resulting matrix (data not shown, see Supplemental Experimental Procedures). C) Receptive fields are estimated using the Gaussian fits in (A) and (B) to match a pixel step size in the LED screen (see Supplemental Experimental Procedures).

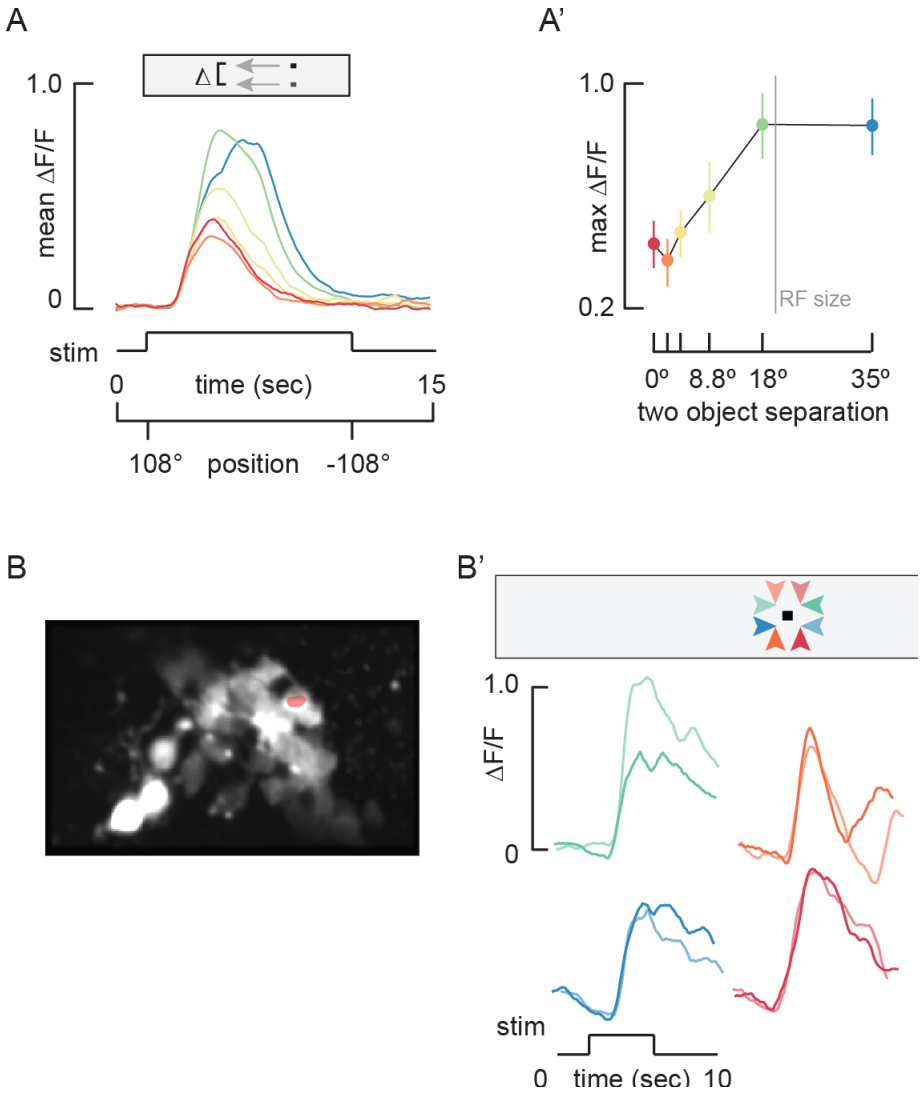

Figure S3 related to Figure 3: LC11 is inhibited by a second object. A and A') Two 8.8° square object moved on parallel trajectories in the back-to-front direction (compare with Figure 3E and3E'). The distance between them was 0°, 2.2°, 4.4°, 8.8°, 18° and 35°, colors mapped to separation distance in C' (n = 6 flies). Vertical gray line indicates average receptive field (RF) size (Figure 3). B and B') A single LC11 is not directionally selective. B) Representative image of the 2-photon imaging plane. Orange region represents the imaged ROI for the data presented in B'. B') Calcium traces from a single cell body presented with an 8.8° by 8.8° object moving 33° deg/sec in 4 cardinal directions. Two trajectories were used for each cardinal direction.

Supplemental Experimental Procedures

Fly Stocks and Histology

Flies were raised on a standard cornmeal diet and kept at 25 °C on a 12 hrs light/ 12 hrs dark cycle. 3-7 day old female flies were used in all experiments. The following fly stocks were used: LC11 was labeled by R22H02-Gal4 (Bloomington ID: #49304), 20XUAS-GCaMP6m (#42748), 10XUAS-GFP (#32185), UAS-DenMark, UAS-syt.EGFP (#33065), pJFRC100-20XUAS-TTS-Shi^{ts1} (attP2, Janelia) and pJFRC49-10XUAS-IVS-eGFPKir2.1 (Janelia), pBDPGal4U ("empty-Gal4", Janelia). Single cell experiments were achieved by crossing R22H02 driver

line to R57C10-Flp2::PEST driving the expression of a multi-color flip out cassette (#64089) and dissecting 2-3 day old flies. To achieve labeling of multiple LC11s with different epitopes we dissected 6-7 day old flies from the same cross. For inactivation experiments following genotypes were used: w-;;R22H02-Gal4/10XUAS-IVS-eGFPKir2.1 and w-;;R22H02-Gal4/pBDPGal4U. We used the following genotype for Figure S4: w-;20XUAS-GCaMP6m/+;R22H02-Gal4/20XUAS-TTS-Shi^{ts1}.

2-5 day old flies were dissected in PBS and fixed in 4% PFA for 25 minutes followed by 3x15 min washes in PBST (0.3% Triton). Brains were then blocked in 5% goat serum for 30 minutes and incubated in primary antibodies for 2 days at 4 °C. This was followed by 3x15 min washes in 0.3% PBST at RT and incubation in secondary antibodies for 2 days at 4 °C. Brains were mounted on glass slides in Vectashield mounting medium and imaged with a Zeiss LSM700 confocal microscope. Images were analyzed using ImageJ and single cells were traced using the simple neurite tracer. Stochastic labeling was done as described in [S1]. We used the following primary and secondary antibodies: mouse nc82 (1:10, Development Studies Hybridoma bank), mouse anti-ChAT (1:25, DSHB), rabbit anti-VGAT (1:100, gift of D. Krantz), rabbit anti-dsRed (1:1000, Clontech #632496), rabbit anti-GFP (1:1000, Invitrogen), rabbit anti-HA (1:300, Cell Signaling Technologies), rat anti-FLAG (1:200, Novus Biologicals), goat anti-mouse AlexaFluor-488 (1:200, Invitrogen), goat anti-rabbit AlexaFluor-488 (1:200,Invitrogen), goat anti-mouse AlexaFluor-568 (1:200, Invitrogen), donkey anti-rabbit AlexaFluor-594 (1:500, Jackson Immuno Research).

Acquired Z-stacks of cell bodies labeled above the dorsal optic peduncle were used to manually count cell bodies. We have identified total of 4-5 cells that have cell bodies in the vicinity of LC11 somata. 2 of these cell bodies belong to a lobula intrinsic neurons (Loi, Figure S1C). This cell type innervate the boundary between layers 3 and 4 in the lobula and overlap with LC11. The overlap region is not extensive and it doesn't cover LC11 innervations in layer 2 and 5. To achieve LC11 specific calcium imaging we mainly targeted LC11 glomerulus in the Ventrolateral Protocerebrum (VLPR). Loi cells also have cell bodies located ventral to LC11 cell bodies which allowed us to target LC11 cell bodies specifically. Lastly, the responses from lobula where LC11 dendrites located and from the optic peduncle where LC11 cell bodies located matched the responses from LC11 glomerulus confirming that our imaging plane was specific to LC11.

Behavior

3- to 6- day old wild type flies were cold anesthetized and glued to a tungsten pin and placed in a 360° by 120° LED arena with each pixel subtending 3.75° at the eye. A white noise method was adapted from prior work [S2] to measure fly's behavioral impulse response to a single display pixel or 2x2 pixel square centered near zero-degree azimuth and zero-degree elevation.

3-4 day old flies carrying either R22H02-Gal4 or empty-Gal4 with UAS-Kir2.1 cold anesthetized and glued to a tungsten pin as described before [S3]. Flies are incubated at room temperature 1-2 hours prior to the experiment. Experiment consisted of 3 stimuli (a 30° by 15° object, 30° by 120° bar and a wide field grating with a spatial frequency of 30°). Each stimulus presented in two directions (clockwise and counter clockwise) and each direction is repeated 8 times. Presentation order was randomized and each presentation consisted of 4 seconds stimulus presentation at 90°/sec. Between each presentation a 30° by 120° bar was presented under closed loop feedback control to ensure that the fly is actively engaging in the visual task and is oriented towards the visual midline. In Note that the bar sweeping across the visual midline is preceded by DWBA and the mean trace continues to rise as the bar moves from front to back (Figure S1J – bar tracking). By contrast, the steering effort in response to the small object crossing midline decreases (Figure S1K – object avoidance). Aside from an overall reduction in response amplitude generated by the empty Gal-4 genetic background, we observed no discernable effect of LC11 block on the qualitative responses to bar, object, or wide-field grating.

Wing beat data collected using Digidata 1440a digitizer and Axoscope 10 (Molecular Devices). Data are imported to MATLAB for offline analysis. Trials from individual flies were averaged and the first data point is subtracted from the averaged responses resulting in a single trace for each experimental condition for each fly. The data is filtered with a 200 Hz low-pass digital Butterworth filter to remove high frequency noise.

Calcium Imaging

Imaging was done as previously described [S3]. Briefly, flies were anesthetized on a cold block and placed in a hole cut from stainless steel shim centered in a custom made acetal holder. The head capsule and thorax were secured to

the shim using UV-activated glue. The proboscis, antennae and legs were immobilized with low melt point beeswax. A small hole was cut with sharpened forceps (Dumont, #5SF) from the head cuticle above the posterior dorsal rim. M1 and M16 muscles were excised and an air sac was removed to enable optical access to the brain. The head was bathed in saline (103mM NaCl, 3mM KCl, 1.5mM CaCl2, 4mM $MgCl_2$, 26mM $NaHCO_3$, 1mM NaH_2PO_4, 10mM trehalose, 10mM glucose, 5mM TES, 2mM sucrose [S4]). Saline was perfused at 1.5 ml/min via a gravity drip system and the bath temperature was kept at 22 °C. LC11 neurons expressing GCaMP6m was imaged using a two-photon excitation scanning microscope (Intelligent Imaging Innovations). Images were acquired at 10 frames/sec, approximately 150X256 pixels with pixel spacing varying between 0.2 to 0.3 microns.

Picrotoxin (PTX) experiments were performed by diluting 1 mM PTX (P1675, Sigma) 100 mM NaCl stock solution in saline with a final concentration of 10 uM PTX. The PTX saline was perfused for 30-40 minutes prior to the imaging experiment. We observed transient responses in the LC11 glomerulus to light increments and decrements generated by turning the LED screen on and off after long periods of PTX perfusion (data not shown). However, these responses were very short by comparison to motion driven responses and could possibly be attributed to the release of inhibition within peripheral visual pathways [S5]

Visual Stimulus

The 96x32 pixel LED display is cylindrical. The fly is placed 78mm from the display. The vertical elevation of the cylinder subtends 63.22 degrees at the eye. Each individual pixel subtends 2.2 degrees in the coronal plane, but the pixels at the top and bottom of the display are further away and thus subtend 1.63 degrees. The maximum apparent size distortion amounts to ¼ of one pixel. Given that our receptive field estimates are greater than the equivalent of 10 pixels on average, an error of ¼ pixel small would not change our results. Indeed, scrutinizing our data we found no relationship between the size of the vertical axis of individual LC11 receptive fields and their vertical elevation in the visual field, as would be expected from systematic over-estimate from uncorrected elevation perspective. For this reason, to our knowledge none of the many labs using this LED display correct for the varying distance to the pixels along the uncurved vertical dimension of the arena.

Object speed was 22 deg/sec for most of the experiments, which at 10Hz frame acquisition allowed the calcium response to be imaged at each display pixel displacement of the stimulus. In order to reduce the duration of one experiment, receptive fields were mapped using an object speed of 33 deg/sec. For each experiment described in the Results, presentation order was randomized and each stimulus condition was presented three times except for the experiments presented in Figure S4 and Figure S3B' which we presented the stimulus once. The LED arena was turned off for 4 seconds between each stimulus condition. In most experiments the visual stimuli were presented in multiple directions but for clarity we present only front-to-back since we show that LC11 is not directionally selective. Experimental details (size, contrast etc.) are written in the figure captions.

In Figure 3B and B' Weber Contrast is calculated by subtracting the light intensity of the object from the background and dividing by the background intensity.

Image Analysis

Acquired images were aligned to the first image using a novel motion correction algorithm [S6] in ImageJ. When, by visual inspection, this method did not sufficiently stabilize in-plane motion we used a slice alignment algorithm that allowed us to choose a specific landmark on the image (ImageJ – Template Matching Plugin). Images that could not be aligned or contained persistent motion artifacts generated by the live fly were discarded. Aligned images were then exported to MATLAB and ROI selection was in accord with the anatomical region that was recorded. For images of the glomerular region, a single ROI was defined by setting a threshold for pixels equal or greater to two-times the mean of the entire image. The fluorescent value at all resultant pixels were summed at each time point and represented as a single time series trace. Cell body and dendritic ROIs were hand picked by either drawing a quadrilateral around dendritic regions, or a polygon around cell bodies. Each trace was then filtered using a Savitzky-Golay filter with a timespan of 150 ms. For each stimulus condition, repeated three trials were averaged and $\Delta F/F$ was calculated by dividing the signal by the mean intensity over the 2 seconds preceding stimulus motion and subtracting 1.

For receptive field mapping experiments, two matrices were generated with each vector representing the time series response of a single cell body to horizontal motion of an 8.8-by-8.8 degree object at each elevation angle, and

vertical motion at each azimuthal angle, respectively. These two matrices were then downsampled to the step size of the stimulus and multiplied together to map the 2-D spatial receptive field. The mean vertical projection and mean horizontal projection were calculated from the multiplied matrices, and 1-D Gaussians were then fit to each of the two projections. Receptive field calculation was stopped and the recording was rejected if any of the fits had R^2 value lower than 0.90. Rejected receptive fields were due to overlap in the imaging frame. These recordings invariably resulted in non Gaussian multi polar GCaMP responses. Receptive fields that passed this criteria were then reconstructed from the Gaussian fits and enclosed by the full-width at 25% maximum.

Supplemental References

S1. Nern, A., Pfeiffer, B.D., and Rubin, G.M. (2015). Optimized tools for multicolor stochastic labeling reveal diverse stereotyped cell arrangements in the fly visual system. Proc. Natl. Acad. Sci. *112*, 201506763.

S2. Theobald, J.C., Ringach, D.L., and Frye, M.A. (2010). Dynamics of optomotor responses in Drosophila to perturbations in optic flow. J. Exp. Biol. *213*, 1366–75.

S3. Aptekar, J.W., Keleş, M.F., Lu, P.M., Zolotova, N.M., and Frye, M.A. (2015). Neurons forming optic glomeruli compute figure-ground discriminations in Drosophila. J. Neurosci. *35*, 7587–99.

S4. Wilson, R.I., Turner, G.C., and Laurent, G. (2004). Transformation of olfactory representations in the Drosophila antennal lobe. Science (80-.). *303*, 366–70.

S5. Freifeld, L., Clark, D. a, Schnitzer, M.J., Horowitz, M. a, and Clandinin, T.R. (2013). GABAergic Lateral Interactions Tune the Early Stages of Visual Processing in Drosophila. Neuron *78*, 1075–1089.

S6. Dubbs, A., Guevara, J., and Yuste, R. (2016). moco: Fast Motion Correction for Calcium Imaging. Front. Neuroinform. *10*, 6.

S7. Fischbach, K.-F., and Dittrich, a P. (1989). The optic lobe of Drosophila melanogaster. I: A. Golgi analysis of wild-type structure. Cell Tissue Res *258*, 441–475.